SUPPLEMENTAL MATERIAL

Online Methods:

Antibodies and reagents

The following commercial antibodies were used: AMPKα1 (#2795, 1:1,000 for Western blot), AMPKα2 (#2532, 1:1,000 for Western blot), phospho-ACC (#11818, 1:1,000 for Western blot), ACC (#3676, 1:1,000 for Western blot), PINK1 rabbit mAb (#6946, 1:1,000 for Western blot), SQSTM1/p62 rabbit mAb (#8025, 1:1,000 for Western blot), LC3A/B rabbit mAb (#12741, 1:1,000 for Western blot), beclin 1 rabbit mAb (#3495, 1:1,000 for Western blot), Atg5 (#12994, 1:1,000 for Western blot), GAPDH (#2118, 1:1,000 for Western blot, CST, Danvers, MA); total OXPHOS WB antibody cocktail (ab110413, 1:1,000 for Western blot), anti-MTCO2 antibody (ab110258, 1:1,000 for Western blot), anti-MT-CYB antibody (ab81215, 1:1,000 for Western blot), anti-MT-ND1 (ab181848, 1:1,000 for Western blot), anti-VDAC1-mitochondrial loading control (ab15895), phospho-AMPKα2 (Thr 172) (ab133448, 1:1,000 for Western blot, Abcam, Cambridge, MA); ANP (sc-20158, 1:1,000 for Western blot), β-MHC (sc-53089, 1:1,000 for Western blot), rabbit control IgG (Sigma-Aldrich). Anti-Parkin (PRK8; Sigma-Aldrich, 1:1,500 for Western blot), phenylephedrine (PE), and ATP Assay Kit (MAK190) were purchased from Sigma-Aldrich (St. Louis, MO, USA); anti-Ubiquitin antibody (05-944) was purchased from Merck Millipore (Darmstadt, Germany). PINK1 plasmid was obtained from Origene Technologies, Inc. (RC206970, Rockville, MD, USA). Ad-AMPKα1 (VH805185) and ad-AMPKα2 (VH801722) were purchased from Vigene Biosciences, Inc. (Rockville, MD, USA). Electron transport chain (ETC) complex I assay kit (A089-1), ETC complex II assay kit (A089-2), ETC complex III assay kit (A089-3) and ETC complex IV assay kit (A089-4) were purchased from Nanjing Jiancheng Bioengineering Institute (Jiangsu, China). Anti-myc (Abcam, #ab9106), Anti-Flag (Sigma-Aldrich, #F7425), recombinant human PINK1 protein (R&D system #AP-180), Anti-Parkin (phospho S65) (Abcam, ab154995), CD90-PE (1:33, Abcam, #ab24904), CD45-FITC (1:10, Biolegend, #103108) and CD31-APC (1:33, Biolegend, #102516) were purchased commercially. The anti-PINK1 (phospho S495) was developed against the antigen peptide QREAS (phos) KRPS (Thermo Fisher Scientific).

Human heart samples

The samples from explanted hearts used in this study were obtained from 5 patients who had received heart transplants (diagnosed as dilated cardiomyopathy [DCM]) at the Tongji Hospital, Tongji Medical College, Huazhong University of Science and Technology and 6 age-matched healthy subjects from traffic accidents. Clinical characteristics of patients are listed in Online Table I. All study participants provided informed written consent and the study was approved by the Institutional Ethics Committee of Tongji Hospital and conducted in accordance with the principles of the Helsinki Declaration. Myocardial posterior wall samples were obtained within 2 h from death or heart transplantation during preparation of donor hearts for transplantation. Immediately after tissue procurement, the samples for biochemical study were stored in liquid nitrogen and kept at −80 °C; samples were later subjected to Western blot, RT-quantitative PCR (RT-qPCR), and respiratory chain enzyme

studies. Selected samples for TEM and immunohistochemical analysis were fixed in 4% paraformaldehyde in phosphate-buffered saline (PBS, pH 7.4), paraffin-embedded, and sectioned.

Echocardiographic analysis

Mice were anesthetized using a mixture of 1.5% isoflurane and O_2 (1–2 L). Echocardiography was performed as described previously[1] with a 30-MHz linear ultrasound transducer.

Hemodynamic measurements of left ventricular function

Measurements of left ventricular function were performed using the Millar catheter system as described previously[2].

Histological analysis and confocal or immunofluorescence microscopy

For histological analysis, hearts were arrested in diastole, perfusion-fixed with 4% paraformaldehyde, embedded in paraffin, and sectioned into 5-μm segments. Paraffin-embedded sections were stained with hematoxylin and eosin (H&E) for routine histological analysis and Masson's trichrome for the detection of fibrillar collagen. Additionally, sections were incubated with primary antibody (LC3 or SQSTM1) for 72 h at 4 °C in a 0.1 N phosphate buffer containing 1% bovine serum albumin (Sigma-Aldrich, A9418) and 1% Triton X-100 (Sigma-Aldrich, X100). After washing with blocking solution, sections were incubated with donkey AlexaFluor-conjugated secondary antibody overnight at 4 °C (Thermo Fisher Scientific, Waltham, MA, USA). Finally, sections were washed and mounted with Prolong Gold Antifade (Thermo Fisher Scientific, P36930). Immunofluorescence images were taken with a Nikon Eclipse E600 microscope or a Zeiss Axiovert 135. Additionally, it was imaged confocally on a Leica SP2 microscope to visualise primary isolated adult mouse cardiomyocytes and then quantified after image processing as described previously[3].

Transmission electron microscopy (TEM)

Heart tissue was removed from the animal and immediately rinsed in PBS. The tissue was placed in a petri dish with 0.5% glutaraldehyde and 0.2% tannic acid in PBS and diced into 2-mm cubes, then transferred to modified Karnovsky's fixative (4% formaldehyde and 2.5% glutaraldehyde containing 8 mM $CaCl_2$ in 0.1 M sodium cacodylate buffer, pH 7.4). Samples were washed with PBS and post-fixed in 1% osmium tetroxide in 0.1 M sodium cacodylate buffer (pH 7.4) for 1 h to produce osmium black. Samples were then dehydrated through a graded series of ethanol and embedded in Epon/SPURR resin (Thermo Fisher Scientific) that was polymerized overnight at 65 °C. Sections of heart tissues and cardiomyocytes were prepared with a diamond knife on a Reichert-Jung Ultracut-E ultra-microtome and stained with UrAc (20 min), followed by 0.2% lead citrate (2.5 min). Images were photographed under an electron microscope. Mitophagy levels (%) of CMs were indicated the number of autophagosomes containing mitochondria per total number of

mitochondria from a cross-sectional assessment of the CMs in TEM.

Mitochondria isolation

Mitochondria were isolated from minced mouse hearts, digested with trypsin, homogenized with a glass/Teflon Potter Elvejhem homogenizer, and then centrifuged at 800 x *g* for 10 min at 4 °C. The supernatant was centrifuged at 8,000 x *g* for 10 min at 4 °C, and the remaining supernatant was discarded. The pellet containing mitochondria was washed and centrifuged at 8,000 x *g* for 10 min at 4 °C before resuspension. Mitochondrial protein concentration was determined by colorimetry using Bio-Rad protein assay dye reagent (500-0006, Bio-Rad, Hercules, CA, USA)[4].

Mitochondrial respiration studies

Mitochondrial respiration (oxygen consumption) was measured in freshly isolated cardiac mitochondria. Myocardial mitochondria from five individual mice were pooled for each experiment. In brief, ventricles were excised, pooled, and washed in ice-cold Chappell-Perry buffer, followed by homogenization. Interfibrillar mitochondria were isolated using differential centrifugation in combination with trypsin digestion. Mitochondrial respiration rates were assessed by measuring oxygen consumption with a Clark-type oxygen electrode at 30 °C. After depletion of endogenous substrates with 100 μmol/L ADP, state 3 respiration rates were recorded in the presence of 100 μmol/L ADP, and state 4 respiration rates were recorded after ADP depletion. ETC enzyme activities were measured spectrophotometrically as specific donor-acceptor oxidoreductase activities using permeabilized mitochondria[5].

Cardiomyocyte culture and treatment

Mouse hearts were removed 5 or 28 days after TAC and perfused using a Langendorff system for ~3 minutes with a Ca^{2+}-free bicarbonate-based buffer. Enzymatic digestion was initiated by adding collagenase type B/D to the perfusion solution. After approximately 7 minutes, the left ventricle was removed and discarded. Cardiomyocytes (CMs) from male mice (8–10 weeks) in the left ventricular wall were isolated as we previously reported[6], and plated at 1–2 × 10^4 cells/cm^2 in mouse laminin pre-coated culture dishes. This technique results in > 95% pure isolated CMs. The cellular survival rate was > 80% at 12 h, and exceeded 65% after 24 h of isolation. After 1 h culture in a 5% CO_2 incubator at 37 °C, CMs were infected with either ad-LacZ or ad-AMPKα2 for 12 h, then subjected to PE (50 μmol/L) stimulation for 24 h, followed by 20 μmol/L carbonyl cyanide p-trichloromethoxyphenyl hydrazone (CCCP) treatment for 8 h. CMs were collected 24 h after PE treatment for Western blotting, ROS production, RT-PCR, ATP levels, flow cytometry, liquid chromatography-tandem mass spectrometry (LC-MS/MS), immunofluorescent staining, and respiratory chain enzyme studies.

Additionally, some experiments were performed using the mouse HL-1 cell line (American type culture collection [ATCC], USA). For experiments such as co-immunoprecipitation, HL-1 cells were treated with PE (0, 10, or 50 μmol/L), and treated

with 20 μmol/L CCCP for 8 h; subsequently, they were subjected to immunoprecipitation with anti-PINK1 antibody to evaluate their interaction with AMPKα1 or AMPKα2. In PINK1 point mutation experiments, HL-1 cells were transfected with PINK1-myc with various mutations, infected with ad-AMPKα2, subjected to SDS–PAGE ± 1,3-bis (bis(pyridin-2-ylmethyl)amino) propan-2-olatodiMn (II) complex (phos-tag), and immunoblotted using anti-PINK1 antibody.

FACS for purification of non-myocyte fraction

Following extraction of primary adult mouse cardiomyocytes, the non-myocyte fraction was resuspended in 100 μL of 5% bovine serum albumin (BSA) / phosphate buffered saline (PBS) solution (137 mmol/L NaCl, 2.7 mmol/L KCl, 1.8 mmol/L KH2PO4, 10 mmol/L Na2HPO4 and 75 μmol/L BSA). Cell isolates were then incubated at 4°C for 20 minutes with CD90-PE (1:33, Abcam, #ab24904), CD45-FITC (1:10, Biolegend, #103108), CD31-APC (1:33, Biolegend, #102516) in 100 μL 5% BSA/PBS. The stained cells were washed in 5% BSA/PBS solution and sorted using a BD FACS ARIA cell sorter. Each purified cell population was centrifuged at 1000 x g for 5 minutes.

ROS Measurement

Isolated adult mouse CMs were suspended in Dulbecco's modified Eagle medium (DMEM) and exposed to PE after adenovirus mediated overexpression of AMPKα2 (ad-AMPKα2). Total ROS production was measured by cytometry with a 2′,7′-dichlorofluorescin diacetate (DCFDA) Cellular ROS Detection Assay Kit (ab113851; Abcam, Cambridge, MA, USA) according to the manufacturer's instructions. Mitochondria-derived ROS levels in CMs were measured using a mitochondrial superoxide indicator (MitoSOX™ Red, M36008; Thermo Fisher Scientific) or by fluorescent staining. In heart sections from WT or AMPKα2$^{-/-}$ mice, ROS production was measured by dihydroethidium (DHE, Sigma-Aldrich) staining.

AMPK activity assays

Protein complexes were isolated by immunoprecipitation using anti-AMPKα1 and -AMPKα2 antibodies. AMPK activity, with purified proteins, was assayed using the SAMS peptide as described previously[7, 8]. The snap-frozen hearts were homogenized, and 100 μg of the lysates were immunoprecipitated with AMPKα1- or α2-specific antibodies. The kinase reaction was performed in the presence of radioactively labeled ATP with synthetic SAMS peptide as the substrate. AMPK activity was expressed as pmol incorporated ATP/mg protein/min.

Autophagy Detection using mRFP-GFP adenoviral vector

Ad-mRFP-GFP-LC3 was purchased from HanBio Technology Co. Ltd. (Shanghai, China); adenoviral infection was performed according to the manufacturer's instructions. Isolated adult mouse CMs were plated in six orifice plates and infected after reaching 50%–70% confluence. Cells were then cultured in DMEM supplemented with 2% FBS with

the adenoviruses at a final multiplicity of infection (MOI) of 60 for 2 h at 37 °C. After infection, cells were grown in medium with 10% FBS and used for further experiments after 36 h. Autophagy was observed under a fluorescence microscope (Nikon Eclipse Ti-s, Japan). Autophagic flux was determined by evaluating the number of GFP and RFP puncta (puncta/cell were counted).

Phos-tag assay

To detect phosphorylated proteins via PAGE, 8% polyacrylamide gels containing 50 μmol/L phos-tag acrylamide (Wako Chemicals, Richmond, VA, USA) and 100 μmol/L $MnCl_2$ were used. After electrophoresis, phos-tag acrylamide gels were washed with transfer buffer containing 0.01% SDS and 1 mmol/L EDTA for 10 min with gentle shaking, and then replaced with transfer buffer containing 0.01% SDS without EDTA for 10 min according to the manufacturer's protocol. Proteins were transferred to polyvinylidene difluoride membranes and analyzed by conventional immunoblotting.

Flow cytometry

Flow cytometry was performed on PE-treated (Sigma-Aldrich, 50 μmol/L for 6 or 24 h) or untreated isolated adult mouse ventricular CMs, in the presence or absence of adenovirus-mediated AMPKα2 (Ad-AMPKα2) overexpression. CMs were then washed in ice-cold PBS, trypsinized, and resuspended in binding buffer containing 10 mmol/L HEPES, pH 7.4, 140 mmol/L NaCl, and 2.5 mmol/L $CaCl_2$. Apoptosis of CMs was measured by double staining with Annexin V-PE and propidium iodide (2.5 mg/mL, Thermo Fisher Scientific). The mitochondrial contents of CMs were measured by MitoTracker™ Deep Red (M22426; Thermo Fisher Scientific) and analyzed using the CellQuest Flow Cytometry System (BD Biosciences, San Jose, CA, USA).

LC-MS/MS analysis of PINK1-myc

PINK1-myc from Ad-LacZ-infected and Ad-AMPKα2-infected CMs was subjected to SDS-PAGE and stained with Coomassie brilliant blue (CBB). PINK1-myc protein bands were excised, reduced, alkylated, and digested with endoproteinase Asp-N (Roche, Basel, Switzerland) in 12.5 mmol/L ammonium bicarbonate and 5 mM Tris-HCl (pH 8.0) for 16 h at 37 °C. The resultant peptides were analyzed on a Q exactive mass spectrometer (Thermo Finnigan, San Jose, CA, USA); the raw data was processed using Xcalibur (Thermo Fisher Scientific). The peak list files were searched against the NCBI nonredundant protein database, restricted to *Homo sapiens*, using the MS/MS ion search function of the Mascot 2.2 search engine (Matrix Science, London, UK).

Adenovirus, plasmid DNA, and short interfering RNA (siRNA)

Transductions with Ad-LacZ, Ad-AMPKα2, Ad-AMPKα1 (Vigene, Rockville, MD, USA), and Ad-GFP-LC3 were carried out for 24 h. Adenoviruses were transduced at 15 MOI.

Human PINK1 mutations (Ser123Ala, Ser199Ala, Ser284Ala, and Ser495Ala) were achieved using the Quick Change Site-Directed Mutagenesis Kit (Stratagene, La Jolla, CA)

with the following primers respectively: Ser123Ala: 3'-GCGGAGAGCCGGCGGGCGGTCGCGGCCTGTCAGGAGATCCA-5' (F), 5'-CGCCTCTCGGCCGCCCGCCAGCGCCGGACAGTCCTCTAGGT-3' (R); Ser199Ala: 3'-AGGGAGAGGCCCAGGTACCGCTGCACCAGGAGAAGGGCAGG-5' (F), 5'-TCCCTCTCCGGGTCCATGGCGACGTGGTCCTCTTCCCGTCC-3' (R); Ser284Ala: 3'-GTTCTCCGCGCCTTCACCTCTGCCGTGCCGCTGCTGCCAGGG-5' (F), 5'-CAAGAGGCGCGGAAGTGGAGACGGCACGGCGACGACGGTCCC-3' (R); Ser495Ala: 3'-CACTGCTCCAGCGAGAGGCCGCCAAGAGACCATCTGCCCGAGT-5' (F), 5'-GTGACGAGGTCGCTCTCCGGCGGTTCTCTGGTAGACGGGCTCA-3' (R). Human PINK1-S495D mutant were generated by point mutation using a site-directed mutagenesis kit (QuikChange II, Stratagene). The siRNA for AMPKα2 and scramble siRNA controls were purchased from Thermo Fisher Scientific. Transfections were performed using Lipofectamine 2000 (Invitrogen, Carlsbad, CA, USA) according to the manufacturer's protocols. GFP-Parkin (PARK2; RG221147; Origene) was subcloned into pCMV6-AC-GFP.

Co-immunoprecipitation and immunoblotting experiments

Mitochondrial or cytosol proteins were extracted from cardiomyocytes and HL-1 cells. Primary antibodies were covalently immobilized on protein A/G agarose using the Pierce Crosslink Immunoprecipitation Kit according to the manufacturer's instructions (Thermo Fisher Scientific). After incubating the cells overnight at 4 °C, 40 µL of protein G-conjugated agarose beads were added, and the solution was incubated for 2 h at 4 °C. The beads were washed five times with PBS and resuspended in 60 µL Laemmli buffer. The immunoprecipitated samples were subjected to immunoblotting using specific primary antibodies and a conformation-specific secondary antibody that recognizes only native IgG (Cell Signaling Technology, Beverly, MA, USA). The precipitates were then analyzed by immunoblotting. For immunoblotting, cell lysates were centrifuged at 13,200 RPM for 15 min at 4 °C. Electrophoresis was performed on Laemmli SDS-polyacrylamide gels. Separated proteins were transferred from the gels to polyvinylidene fluoride membranes by semi-dry electrotransfer, and immunoblotting was performed as previously described[9].

Cell-free kinase assay of recombinant functional AMPKα2β2γ1

Recombinant functional AMPKα2β2γ1 heterotrimers (Sigma Aldrich, catalog number #SRP5003) expressed in Escherichia coli[10, 11] and commercial human PINK1 (R&D system, AP-180) were used for cell-free kinase assay. For activation of recombinant human PINK1, 0.5 mg PINK1 was incubated with commercial human functional AMPKα2β2γ1 or BSA for 30 min or 60 min at 30 °C in activation buffer (10 mmol/L HEPES (pH 7.5), 5 mmol/L $MgCl_2$, 1 mmol/L AMP, 2 mmol/L ATP) as indicated[12]. At incubation for 60 min, lambda phosphatase (λ-phosphatase), an enzyme that releases phosphate groups from phosphorylated serine, threonine and tyrosine residues in proteins, was added in activation buffer. The reaction was stopped by adding SDS loading buffer. Samples were boiled for 5 min and separated by SDS-PAGE, followed by Western blot analysis with the p-PINK1 S495, PINK1 and AMPKα2 antibody.

Quantification of mRNA by reverse transcriptase quantitative PCR (RT-qPCR)

Total RNA was extracted from myocardial tissues in mice and isolated adult mouse CMs using Trizol (Life Technologies Inc., Carlsbad, California, USA). mRNA expression levels for *Cytb, Drp1, FIS1, MFN1, MFN2, PGC1-α, PGC1-β, ULK1, Mt-CO1, Mt-CO2, PINK1, Parkin, ANP, BNP, β-MHC, ACTA1,* and *GAPDH* were quantified by a real-time two-step RT-qPCR assay (GeneAmp7900, HT Applied Bio systems, Foster City, CA). All samples were processed in triplicate and underwent 40 rounds of amplification under the following conditions: 40 cycles of a two-step PCR (95 °C for 30 s, 58 °C for 30 s) after initial denaturation (95 °C for 5 min). A melting curve was also performed to check for off-target amplification. For accurate gene expression measurements, the sequences of primers used for PCR amplification are shown in Online Table II. GAPDH was used as a reference endogenous gene to normalize the results. Each RT-qPCR experiment was performed on at least four different experimental samples.

Online Figure I:

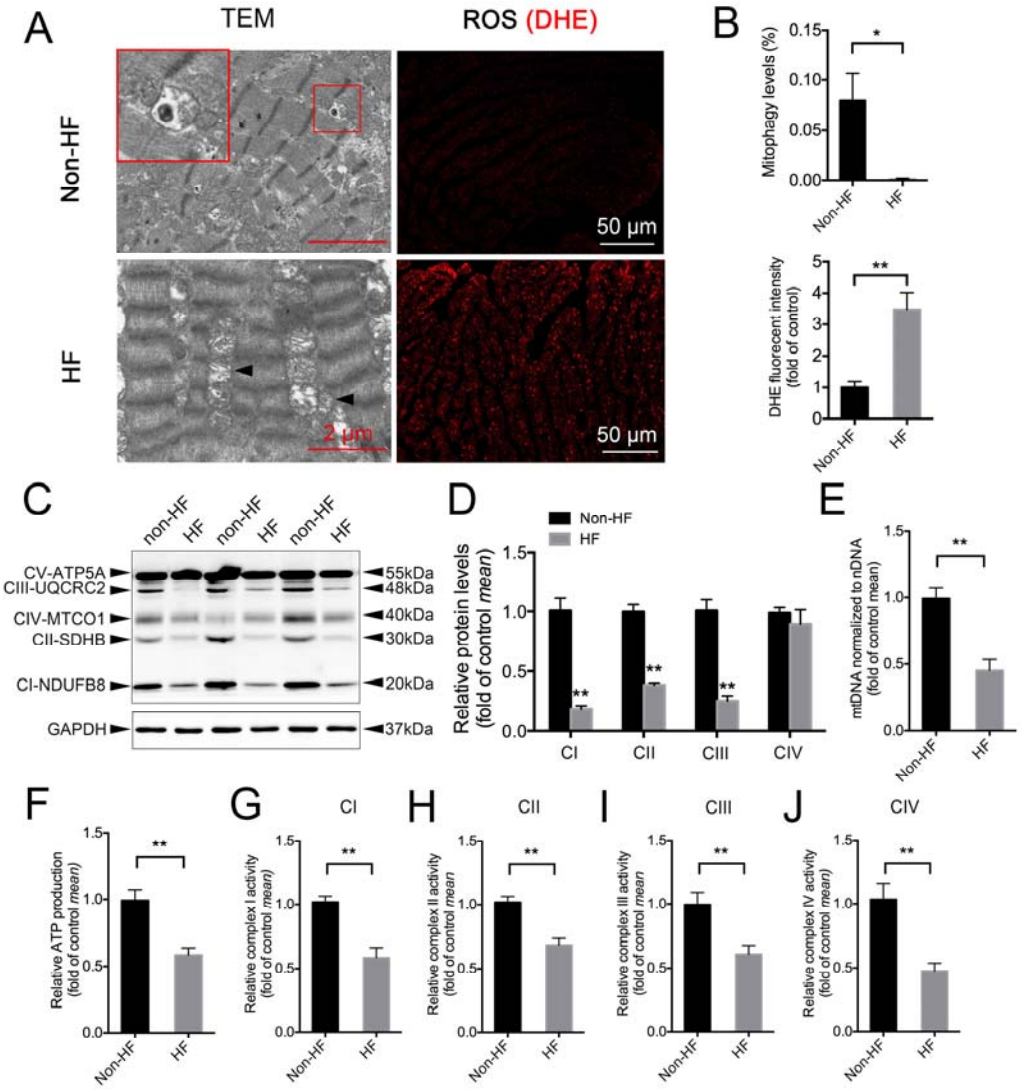

Online Figure I: Mitochondrial abnormality and dysfunction occurred in patients with severe heart failure (HF).

A. Representative images of TEM and DHE staining of myocardial samples from control (non-HF) hearts (n = 6) and hearts from patients with severe HF (n = 5). **B.** Upper, rates of mitophagy in cardiac tissue, bar graphs indicating the number of autophagosomes containing mitochondria per total number of mitochondria from a cross-sectional assessment of the heart tissues in TEM, $^{*}P < 0.05$ vs non-HF patients. Bottom, quantitative DHE mean fluorescent intensity. $^{**}P < 0.01$ vs non-HF patients. **C.** Protein extracts of myocardial samples from control hearts and hearts from patients with severe heart failure were normalized to equal protein levels. Representative bands of ETC complex proteins in Western blot are shown. **D.** Relative ETC complex protein levels; CV-ATP5A was used as a control. $^{**}P < 0.01$ vs non-HF patients. **E.** Myocardial mitochondrial DNA (mtDNA) levels in human. $^{**}P < 0.01$ vs non-HF patients. **F.** Myocardial ATP levels in human. $^{**}P < 0.01$ vs non-HF patients. **G–J.**

ETC complex (I–IV) activity in human heart was examined by an enzyme-linked immunosorbent assay (ELISA). $^{**}P < 0.01$ vs non-HF patients. All data represent the mean ± SEM.

Online Figure II:

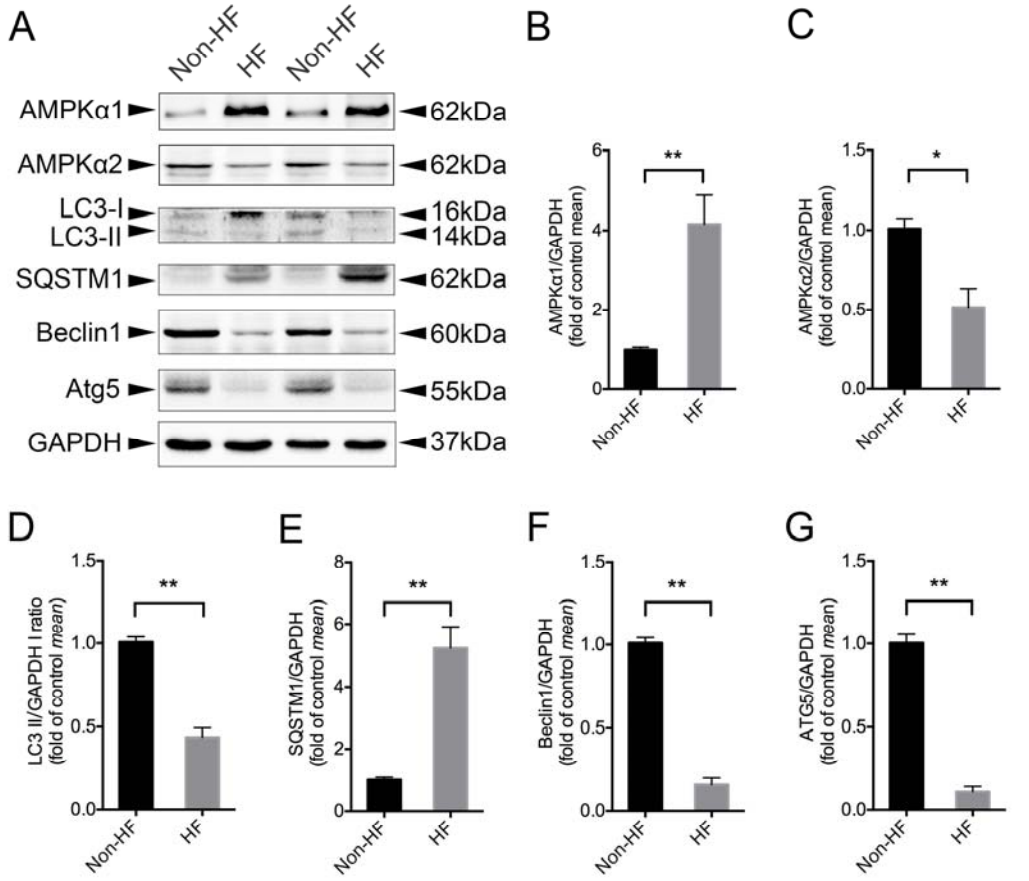

Online Figure II: General autophagy level was reduced in patients with severe HF, and severe HF was associated with AMPKα1 and AMPKα1 isoform switch.

A. Representative immunoblots of whole-cell heart homogenates from control (non-HF) hearts (n = 6) and hearts from patients with severe HF (n = 5). **B.** Quantitative analysis of AMPKα1 expression in heart. $^{**}P < 0.01$ vs non-HF patients. **C.** Quantitative analysis of AMPKα2 expression in heart. $^{*}P < 0.05$ vs non-HF patients. **D.** Quantitative analysis of LC3II expression in heart. $^{**}P < 0.01$ vs non-HF patients. **E.** Quantitative analysis of SQSTM1 expression in heart. $^{**}P < 0.01$ vs non-HF patients. **F.** Quantitative analysis of Beclin1 expression in heart. $^{**}P < 0.01$ vs non-HF patients. **G.** Quantitative analysis of Atg5 expression in heart. $^{**}P < 0.01$ vs non-HF patients. All data represent the mean ± SEM from at least four independent experiments.

Online Figure III:

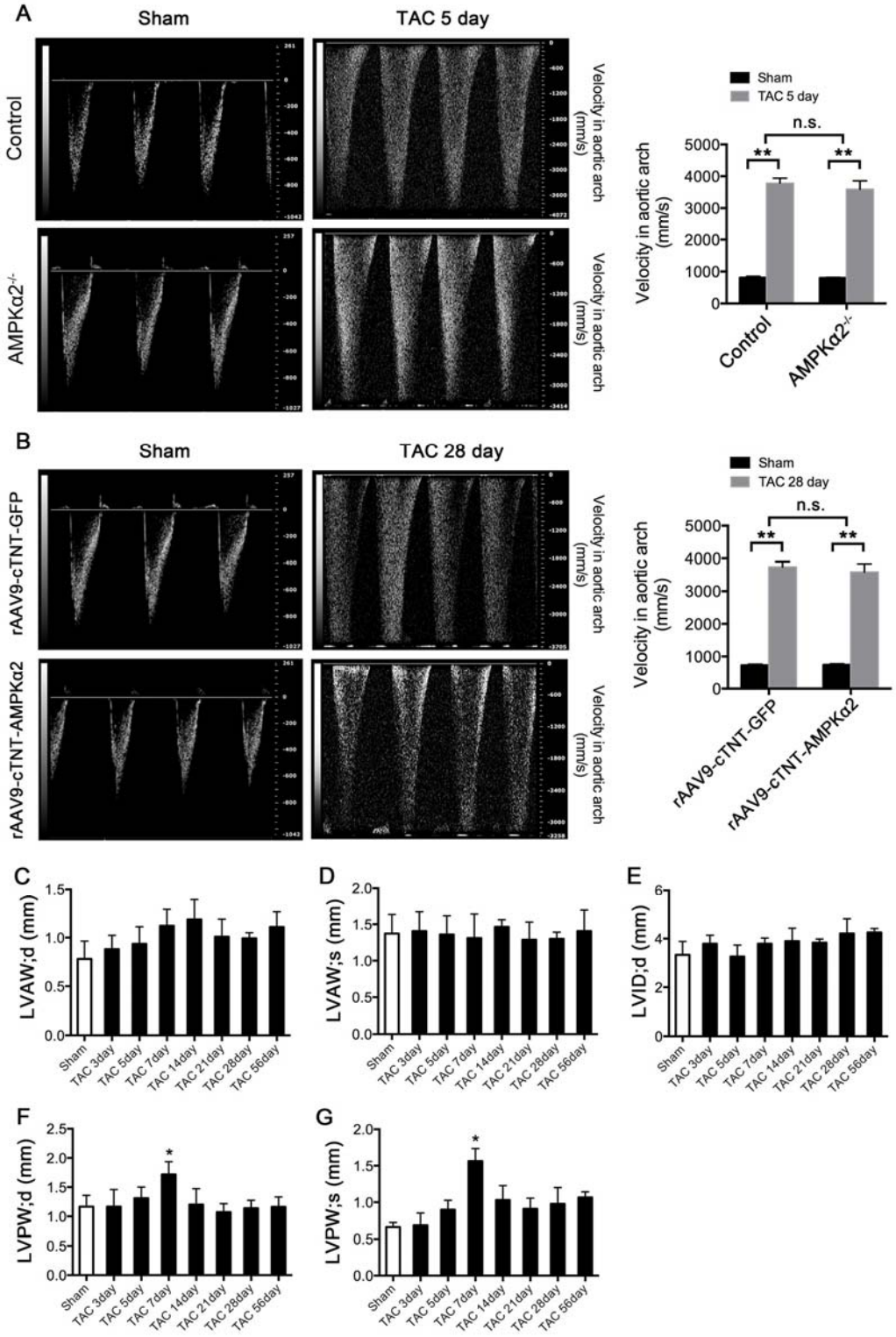

Online Figure III: Echocardiographic analysis of C57BL/6J mice.

A. AMPKα2$^{-/-}$ mice and control littermates were subjected to either sham operation (n = 10 in littermates control group, n = 12 in AMPKα2$^{-/-}$ group) or TAC for 5 days (n = 12 in

littermates control group, n = 14 in AMPKα2$^{-/-}$ group). Representative images of echocardiography and quantitative analysis of velocity in mice aortic arches are shown, $^{**}P < 0.01$ vs. sham group in WT or AMPKα2$^{-/-}$ mice, respectively. **B.** C57BL/6J mice were first injected with rAAV9-cTNT-AMPKα2 in the caudal vein; rAAV9-cTNT-GFP was used as a control. After 2 weeks, infected mice were subjected to either sham operation (n = 20 in rAAV9-cTNT-AMPKα2 group; n = 20 in rAAV9-cTNT-GFP group) or TAC for 28 days (n = 25 in rAAV9-cTNT-AMPKα2 group; n = 25 in rAAV9-cTNT-GFP group). Representative images of echocardiography and quantitative analysis of velocity in mice aortic arches are shown, $^{**}P < 0.01$ vs sham group in rAAV9-cTNT-GFP or rAAV9-cTNT-AMPKα2 mice, respectively. **C.** Left ventricular diastolic anterior wall in diastole (LVAWd). **D.** Left ventricular systolic anterior wall in systole (LVAWs). **E.** Left ventricular internal diameter in diastole (LVIDd). **F.** Left ventricular diastolic posterior wall in diastole (LVPWd). $^{*}P < 0.05$ vs sham operations. **G.** Left ventricular systolic posterior wall in systole (LVPWs). $^{*}P < 0.05$ vs sham operations.

Online Figure IV:

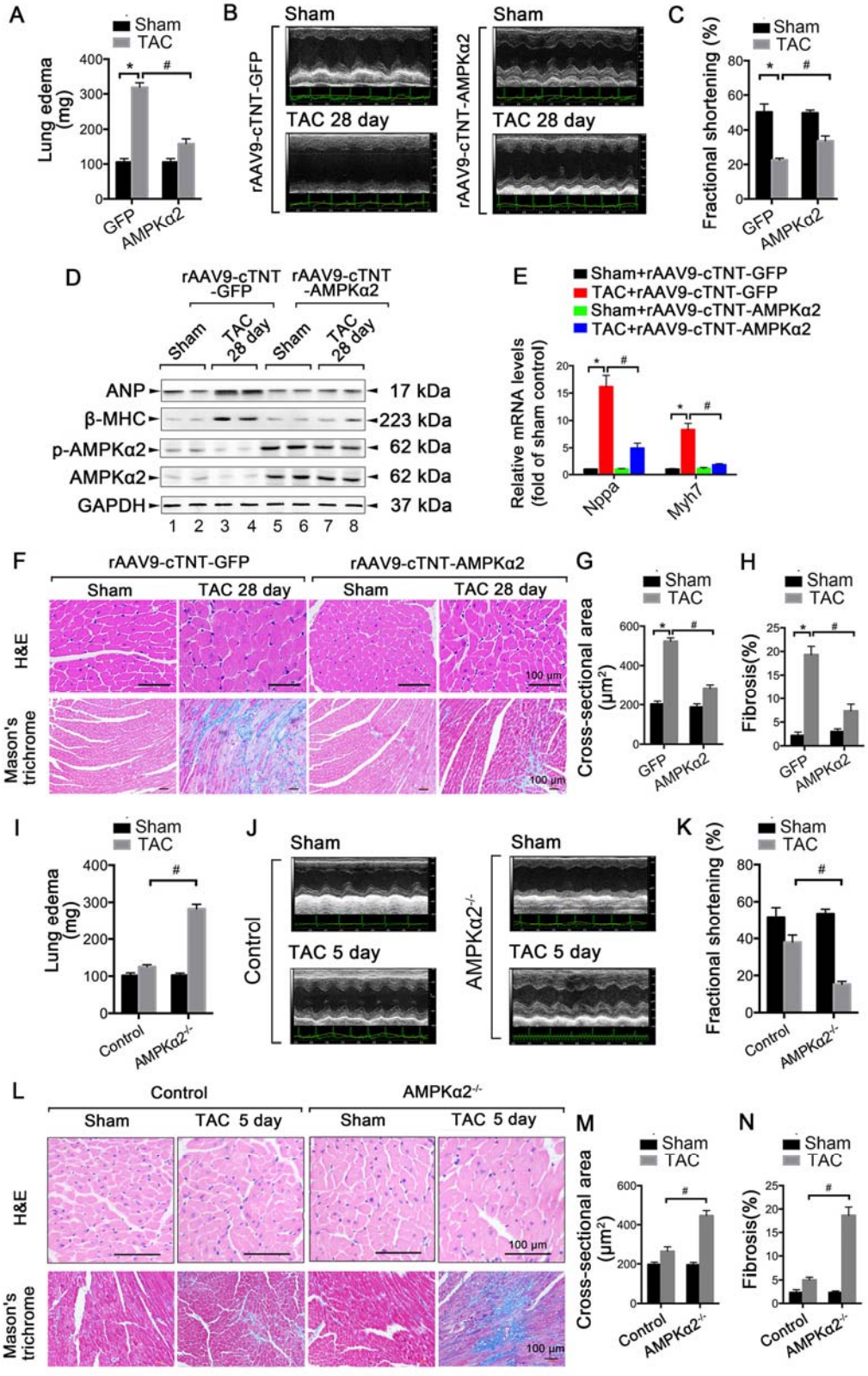

Online Figure IV: Gain- and loss-of-function of AMPKα2 altered the development of HF in

TAC-induced mice.

C57BL/6J mice were first injected with rAAV9-cTNT-AMPKα2 or rAAV9-cTNT-GFP (control) in the caudal vein. After 2 weeks, infected mice were subjected to either sham operation (n = 20 in rAAV9-cTNT-AMPKα2 group, n = 20 in rAAV9-cTNT-GFP group) or TAC for 28 days (n = 25 in rAAV9-cTNT-AMPKα2 group, n = 25 in rAAV9-cTNT-GFP group). **A.** Lung edema index (wet lung weight – dry lung weight) at 28 days after TAC or sham surgery in AMPKα2 overexpression or GFP groups. $^{*}P<0.05$ vs sham group; $^{\#}P<0.05$ vs TAC in GFP group. **B.** Representative images of echocardiograms. **C.** LV fractional shortening, $^{*}P<0.05$ vs sham group, $^{\#}P<0.05$ vs TAC in GFP group. **D.** Representative immunoblots of ANP, β-MHC, p-AMPKα2 and AMPKα2 proteins in lysates prepared from heart homogenates (n=4 for each group). **E.** RT-PCR analyses of relative expression of *nppa* and *myh7* genes from the hearts of mice exposed to the indicated conditions (n=4 for each group). **F.** Representative images of H&E and fibrosis staining in mice heart sections. Scale bar, 100 μm. **G.** Quantification of the size of CMs by measurement of the cross-sectional area on H&E-stained sections. $^{*}P < 0.05$ vs sham operations; $^{\#}P < 0.05$ vs TAC operations. **H.** Masson trichrome staining of adult mice hearts sections. Quantification of the rate of cardiac fibrosis by measurement of the area of collagen deposition was shown. $^{*}P < 0.05$ vs sham operations; $^{\#}P < 0.05$ vs TAC operations. **I.** AMPKα2$^{-/-}$ mice, and littermates, were subjected to either sham operation or TAC for 5 days. Lung edema index (wet lung weight – dry lung weight) at 5 days after TAC or sham surgery. $^{*}P<0.05$ vs sham group; $^{\#}P<0.05$ vs TAC in control group. **J.** Representative images of echocardiograms. **K.** LV fractional shortening, $^{*}P<0.05$ vs sham group; $^{\#}P<0.05$ vs TAC in control group. **L.** Representative images of H&E and Masson's trichrome staining of heart sections from mice after sham operation (n = 5) or 5 days after TAC (n = 6). **M.** Quantification of the size of CMs by measuring the cross-sectional area on H&E-stained sections. $^{*}P < 0.05$ vs sham group; $^{\#}P < 0.05$ vs TAC in control group. **N.** Masson's trichrome staining of adult mice hearts sections. Quantification of the rate of cardiac fibrosis by measurement of the area of collagen deposition is shown. $^{*}P < 0.05$ vs. sham group; $^{\#}P < 0.05$ vs TAC in control group.

Online Figure V:

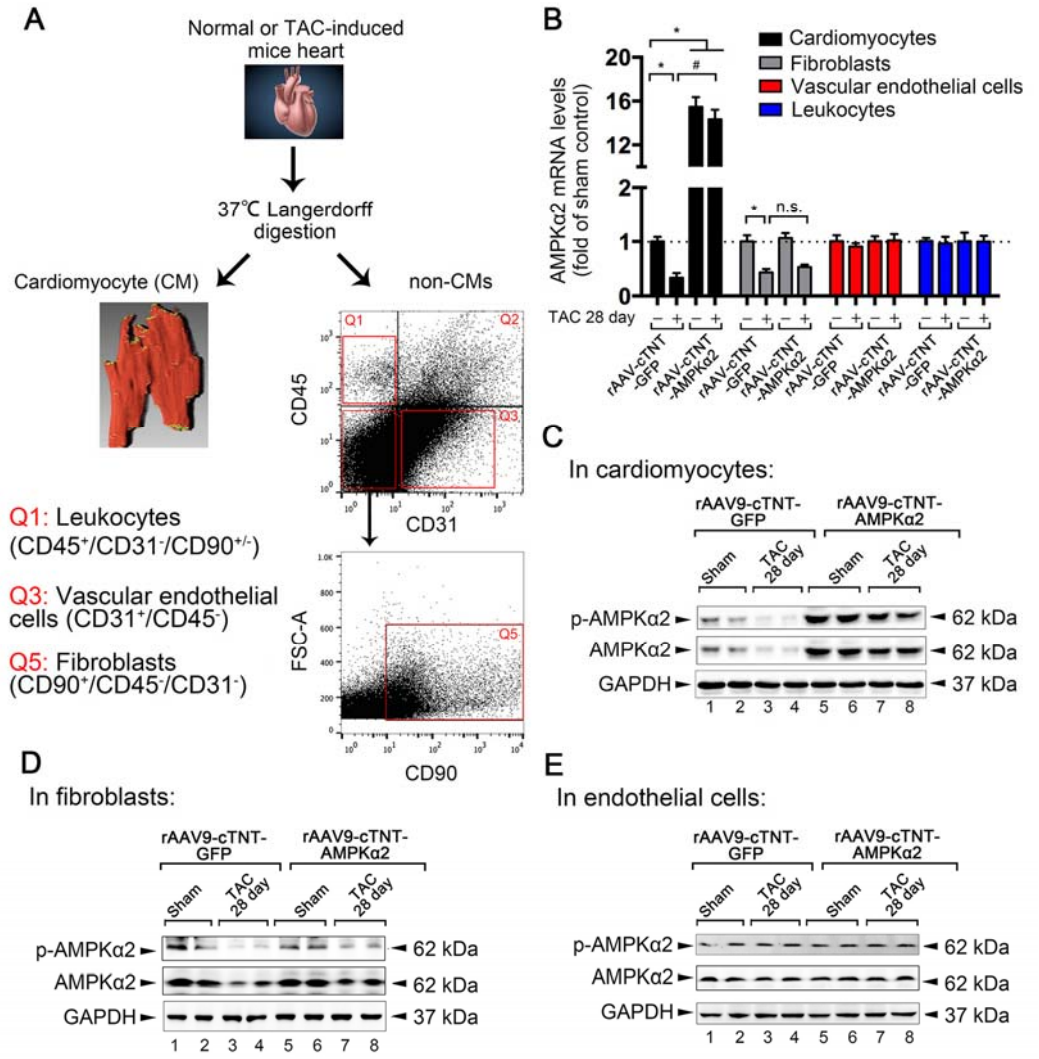

Online Figure V: Isolation of primary adult mouse CMs and purification of non-myocyte fraction by FACS.

C57BL/6J mice were first injected with rAAV9-cTNT-AMPKα2 or rAAV9-cTNT-GFP (control) in the caudal vein. After 2 weeks, infected mice were subjected to either sham operation (n = 20 in rAAV9-cTNT-AMPKα2 group, n = 20 in rAAV9-cTNT-GFP group) or TAC for 28 days (n = 25 in rAAV9-cTNT-AMPKα2 group, n = 25 in rAAV9-cTNT-GFP group). **A.** Schematic of cardiac cell sorting strategy. **B.** Quantitative mRNA levels of AMPKα2 after TAC for 28 days in presence of rAAV9-cTNT-AMPKα2 or control in multi-cells in heart. $^{*}P < 0.05$ vs sham group; $^{\#}P < 0.05$ vs TAC in control group. **C.** Representative immunoblots of p-AMPKα2 and AMPKα2 in isolated adult mouse CMs. **D.** Representative immunoblots of p-AMPKα2 and AMPKα2 in isolated adult mouse fibroblasts. **E.** Representative immunoblots of p-AMPKα2 and AMPKα2 in isolated adult mouse vascular endothelial cells. All data represent the mean ± SEM from at least four independent experiments.

Online Figure VI:

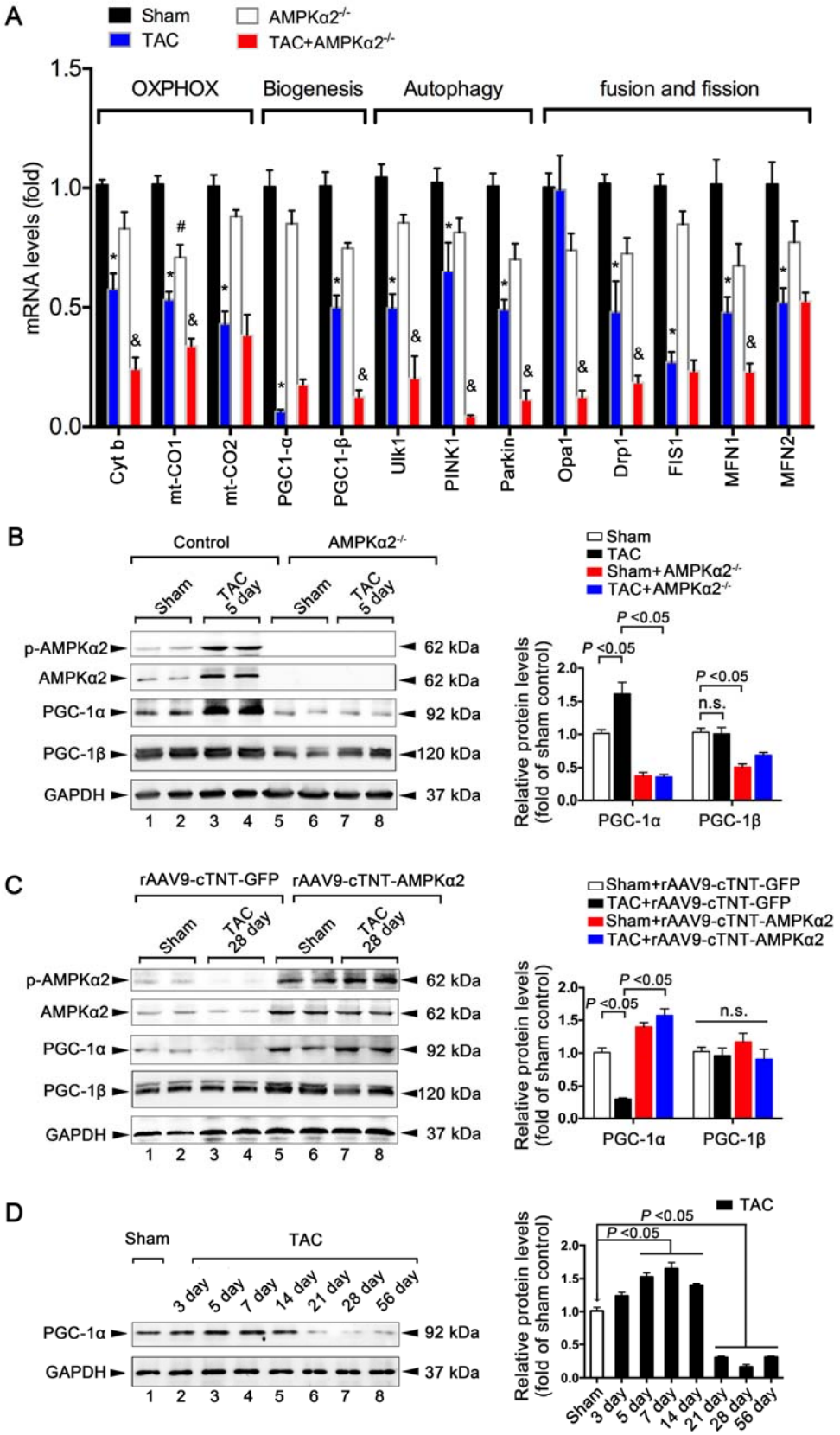

Online Figure VI: Gain- and loss-of-function of AMPKα2 influence mitochondrial biogenesis via PGC-1α during development of HF in TAC-induced mice.

A. AMPKα2$^{-/-}$ mice, and littermates, were subjected to either sham operation (n = 12 for AMPKα2$^{-/-}$ group, n = 10 in littermates control group) or TAC for 5 days (n = 14 in AMPKα2$^{-/-}$ group, n = 12 in littermates control group). RT-qPCR analysis for cardiac metabolic and mitochondrial genes. $^{*}P < 0.05$ vs sham group; $^{\&}P < 0.05$ vs TAC group. **B-C.** Representative immunoblots of PGC-1α, PGC-1β, p-AMPKα2 and AMPKα2 in lysates prepared from heart homogenates; GAPDH was used as the loading control (n = 4 for each group). **D.** Representative immunoblots of PGC-1α in the fraction prepared from heart homogenates after TAC for different days; GAPDH was used as the loading control (n = 4 for each group). All data represent the mean ± SEM from at least four independent experiments.

Online Figure VII:

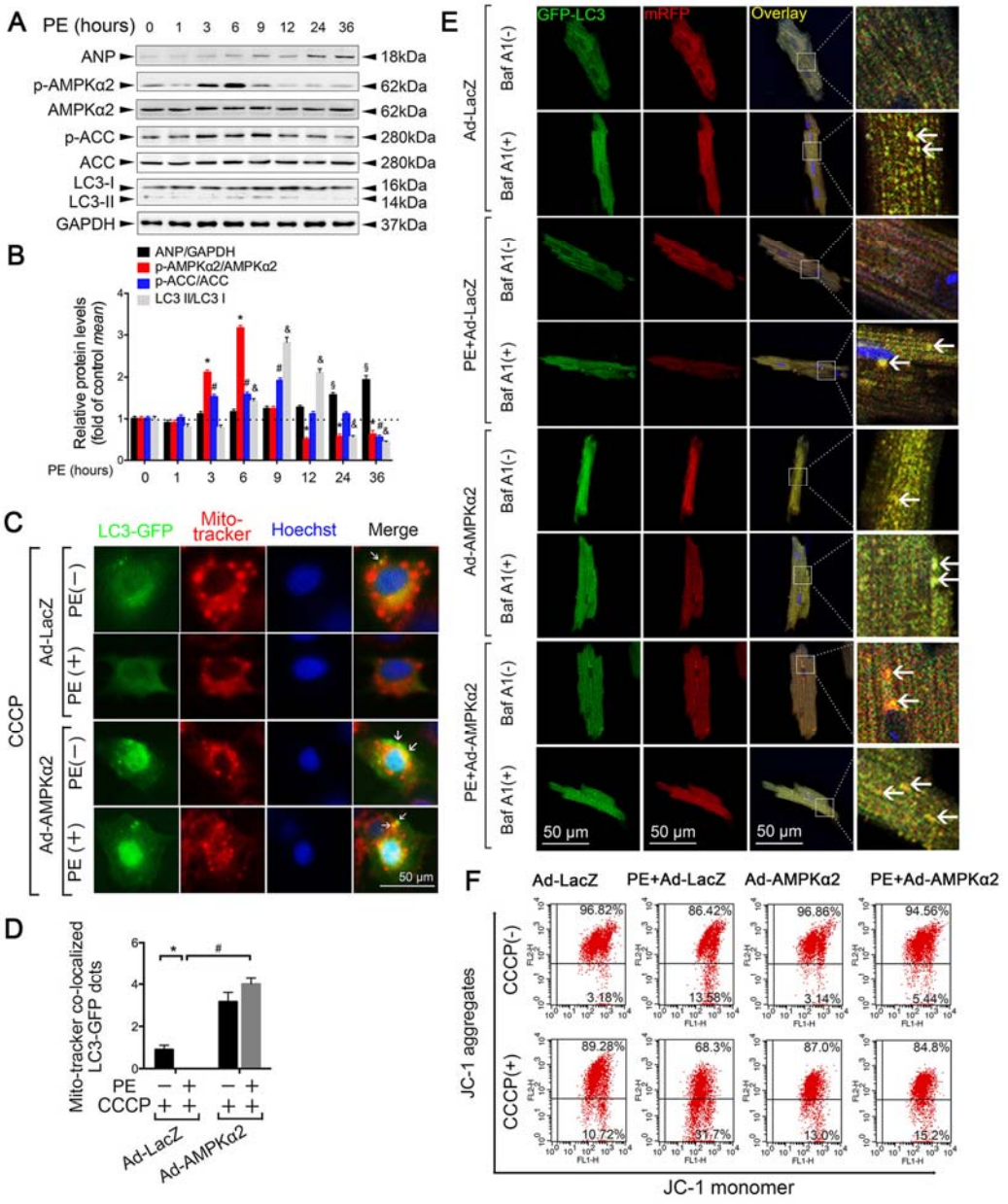

Online Figure VII: Autophagy and autophagic flux in PE-induced CMs.

A. Isolated mouse adult CMs were treated with PE (50 μmol/L) stimulation at different time points. Representative immunoblots of ANP, p-AMPKα2, AMPKα2, p-ACC, ACC, LC3, and GAPDH in lysates from PE-induced CMs are shown. **B.** Quantification of ANP/GAPDH ($^{\S}P < 0.05$ vs control group), p-AMPKα2/AMPKα2 ($^{*}P < 0.05$ vs control group), p-ACC/ACC ($^{\#}P < 0.05$ vs control group), and LC3-II/LC3-I ($^{\&}P < 0.05$ vs control group). **C.** The degree of colocalization of mitochondria (mitotracker, red) with GFP-LC3 in mouse HL-1 cells was measured via live cell imaging microscopy. **D.** Bar graphs indicate the number of colocalization of mitochondria (mitotracker, red) with GFP-LC3 per cell. *P<0.05 vs Ad-LacZ group, #P<0.05 vs. PE+Ad-LacZ group. **E.** Enlargement of Figure 5**I.**

Representative images of mRFP-GFP-LC3 puncta are shown. Chloroquine (chl) was injected (10 mg/kg) intraperitoneally. Scale bar, 50 μm. **F.** Enlargement of Figure 5**C.** Mitochondrial membrane potential was examined by flow cytometry with JC-1 probe treatment. A loss of mitochondrial membrane potential (ΔΨm) was demonstrated by the change in JC-1 fluorescence from red (JC-1 aggregates) to green (JC-1 monomers). All data represent the mean ± SEM from at least four independent experiments.

Online Figure VIII:

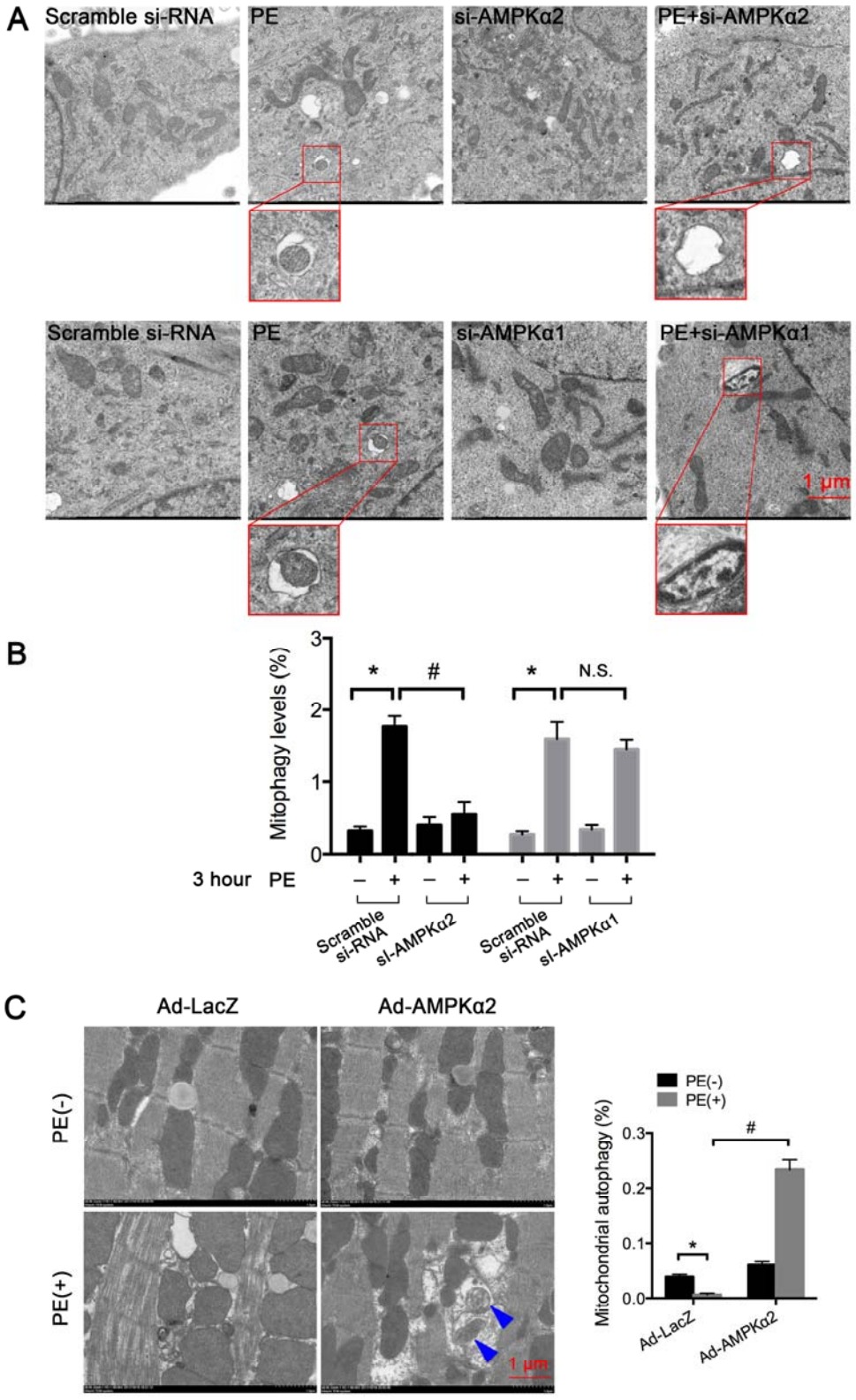

Online Figure VIII: Mitophagy levels after AMPKα loss-of-function in PE-induced CMs.

A. Mouse HL-1 CMs were disrupted with si-AMPKα2 or si-AMPKα1, and then treated with PE (50 μmol/L, 6 h). Representative images of TEM are shown. **B.** Mitophagy levels in CMs after indicated interventions. Bar graphs indicate the number of autophagosomes containing mitochondria per total number of mitochondria from a cross-sectional assessment of the CMs in TEM. $^{*}P < 0.05$ vs. scramble si-RNA control group; $^{\#}P < 0.05$ vs. PE+scramble si-RNA group. N.S. = No significance. **C.** Mitophagy levels in isolated adult mouse CMs subjected to PE and transfection with ad-AMPKα2. $^{*}P < 0.05$ vs. ad-LacZ; $^{\#}P < 0.05$ vs. ad-LacZ+PE. Blue arrow indicates the autophagosomes containing mitochondria. All data represent the mean ± SEM from at least four independent experiments

1

Online Figure IX:

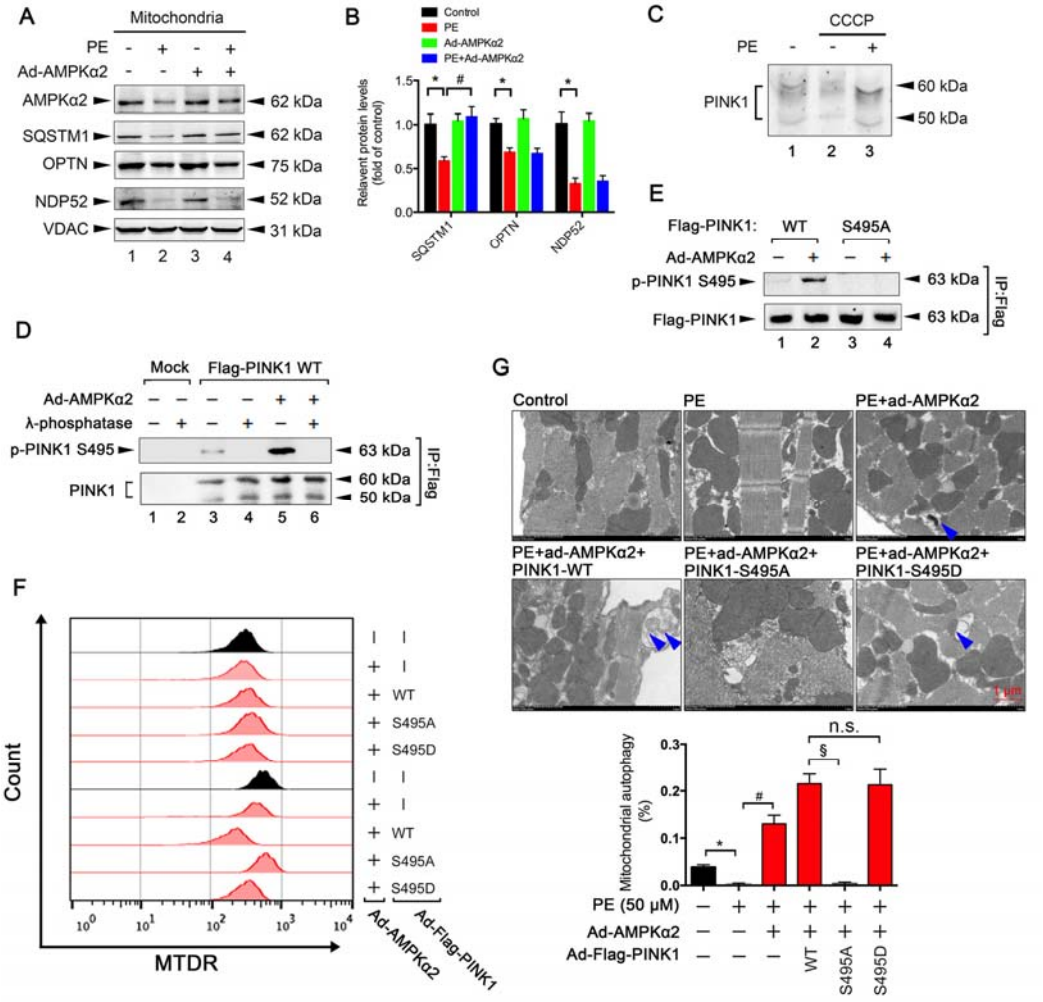

Online Figure IX: PINK1 mobility decreased after PE stimulation in CMs.

A. Isolated mouse adult CMs were infected with adenovirus encoding AMPKα2, then subjected to PE (50 μmol/L, 24 h) stimulation. Representative immunoblots of AMPKα2, SQSTM1, OPTN, and NDP52 in lysates of mitochondrial fractions in CMs. VDAC1 was used as the loading control. **B.** Quantification of SQSTM1, OPTN, and NDP52 relative to VDAC1. $^{*}P < 0.05$ vs. control group; $^{\#}P < 0.05$ vs PE group. **C.** Isolated mouse adult CMs were subjected to PE (50 μmol/L, 24 h) stimulation, followed by treatment with 20 μmol/L CCCP for 8 h. Endogenous PINK1 mobility was examined by Western blotting. Results were replicated in four independent experiments. **D-E.** Examination for phosphorylation of PINK1 by using p-PINK1 S495 antibody in HL-1 CMs. **F.** Enlargement of Figure 8**K. G.** Isolated mouse adult CMs were infected with adenovirus encoding AMPKα2 and plasmid containing PINK1 (WT, S495A or S495D), then subjected to PE (50 μmol/L, 24 h) stimulation. TEM analysis for mitochondrial autophagy levels, $^{*}P < 0.05$ vs control group; $^{\#}P < 0.05$ vs. PE group; $^{\S}P < 0.05$ vs. (PE+ ad-AMPKα2+PINK1-WT) group. All data represent the mean ± SEM from at least four independent experiments.

Online Figure X:

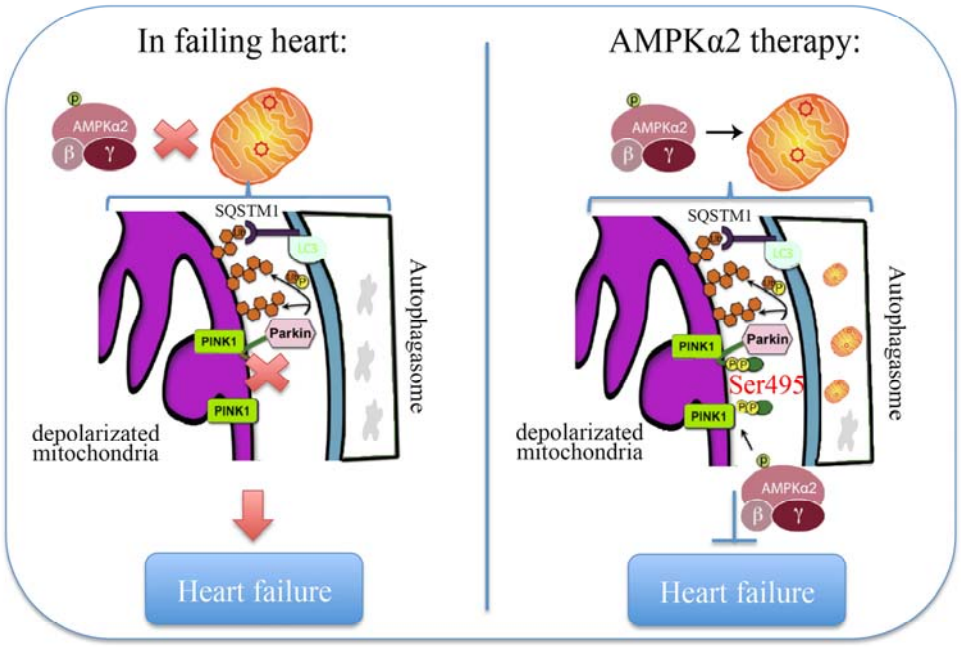

Online Figure X: Proposed model for the signaling pathway by which AMPKα2 increases mitophagy to prevent HF.

In failing hearts, the dominant AMPKα isoform switched from AMPKα2 to AMPKα1. The suppression of AMPKα2 activity resulted in an impairment of mitophagy in the heart and accelerated progression to HF. Overexpression of AMPKα2 rescued the impairment of mitophagy by phosphorylating PINK1 at Ser495 to enhance the PINK1-Parkin-SQSTM1 pathway; damaged mitochondria were removed and mitochondrial functions improved. Thus, AMPKα2 therapy prevents HF by phosphorylating PINK1 at Ser495 and increasing mitophagy.

Online Table I:

Online Table I. Clinical characteristics of Non-HF and HF patients

Patient	Age	Gender	Diagnosis	NYHA	LVEF%	LVEDD (mm)
HF 1	46	Male	DCM	4	16	62
HF 2	40	Female	DCM	3	21	60
HF 3	49	Male	DCM	4	19	65
HF 4	54	Female	DCM	4	15	68
HF 5	39	Male	DCM	4	18	55
Non-HF 1	45	Male	Normal	N/A	68	50
Non-HF 2	56	Female	N/A	N/A	72	N/A
Non-HF 3	62	Male	N/A	N/A	79	N/A
Non-HF 4	55	Female	Normal	N/A	82	49
Non-HF 5	46	Female	Normal	N/A	76	48
Non-HF 6	50	Male	Normal	N/A	81	49

Non-HF, non-heart failure; HF, heart failure; DCM, dilated cardiomyopathy; NYHA, New York Heart Association function class; LVEF, left ventricular ejection fraction; LVEDD, left ventricular end-diastolic dimension.

Online Table II:

Online Table II. Primers for quantitative real-time PCR

Gene name	Gene ID	Forward or 5' primer	Reverse or 3' primer
Cytb	NC_005089.1	TTCTGAGGTGCCACAGTTATT	GAAGGAAAGGTATTAGGGCTAAA
Drp1	NC_000082.6	TGCAGCTAGTCCACGTTTCA	CCCATTCTTCTGCTTCAACTCT
FIS1	NM_025562.3	TGGTGTCTGTGGAGGATCTG	ATTGCGTGCTCTTGGACAC
MFN1	NM_024200.4	AAGCATAAAGCTCAGGGGATG	TGCTTGAAATCCTTCTGCAA
MFN2	NM_133201.2	CACAGTGGGTCACGTGAAAA	CCCCCAGAAAGAACACAACA
PGC1-α	NM_008904.2	GAAAGGGCCAAACAGAGAGA	GTAAATCACACGGCGCTCTT
PGC1-β	NC_000084.5	GACGTGGACGAGCTTTCACT	CTGCTGTTCCGTCAACTCAA
ULK1	NM_009469.3	GGATCCATGGTGTCACTGC	CAAGGGCAGCTGATTGTACC
Mt-CO1	NC_005089.1	CAGACCGCAACCTAAACACA	TTCTGGGTGCCCAAAGAAT
Mt-CO2	NC_005089.1	GCCGACTAAATCAAGCAACA	CAATGGGCATAAAGCTATGG
PINK1	NM_026880.2	GCTTGCCAATCCCTTCTATG	CTCTCGCTGGAGCAGTGAC
Parkin	NC_000083.5	GAGATGGTGTGACAAGGGGAATGAGAAG	CCCCTGTCGCTTAGCAACCACTTC
ANP	NM_008725.2	AGTGCGGTGTCCAACACAGAT	TCCTTGGCTGTTATCTTCGGTA
BNP	NM_008726.4	CCTAGCCAGTCTCCAGAGCAAT	CTTCCTACAACAACTTCAGTGCGT
β-MHC	NM_080728.2	CTACAGGCCTGGGCTTACCT	TCTCCTTCTCAGACTTCCGC
ACTA1	NM_001272041.1	CTAGACACACTCCACCTCCA	GTCAGTTTACGATGGCAGCA
GAPDH	NM_008084.2	CAAAATGGTGAAGGTCGGTGTG	TGATGTTAGTGGGGTCTCGCTC

Online Table III. Phosphopeptides identified by LC-MS/MS. The top 10 phosphopeptides were listed according to PINK1+ad-AMPKα2 group. The phosphorylated residues are indicated in color red.

Accession	Description	Peptides	Vector group		PINK1-WT+Ad-LacZ group		PINK1-WT+ad-AMPKα2 group		PINK1-WT+si-AMPKα2 group	
			Residue	Modification	Residue	Modification	Residue	Modification	Residue	Modification
Q9BXM7	PINK1_HUMAN Serine/threonine-protein kinase PINK1, mitochondrial OS=Homo sapiens GN=PINK1 PE=1 SV=1	[488] ALLQREASK [496]	S495		S495		S495	PHOS	S495	
P02765	FETUA_HUMAN Alpha-2-HS-glycoprotein OS=Homo sapiens GN=AHSG PE=1 SV=1	[132] CDSSPDSAEDVR [143]	S134		S134		S134	PHOS	S134	
Q92945	FUBP2_HUMAN Far upstream element-binding protein 2 OS=Homo sapiens GN=KHSRP PE=1 SV=4	[267] MILIQDGSQNTNVDKPLR [284]	S274	PHOS	S274	PHOS	S274	PHOS	S274	PHOS
P22090	RS4Y1_HUMAN 40S ribosomal protein S4, Y isoform 1	[54] YALTGDEVK [62]	T57		T57		T57	PHOS	T57	

Q9BXM7	OS=Homo sapiens GN=RPS4Y1 PE=1 SV=2 PINK1_HUMAN Serine/threonine-protein kinase PINK1, mitochondrial OS=Homo sapiens GN=PINK1 PE=1 SV=1	[280] AFTSSVPLLPGAL VDYPDVLPSR [302]	S284		S284		S284	PHOS	S284	
Q9BXM7	PINK1_HUMAN Serine/threonine-protein kinase PINK1, mitochondrial OS=Homo sapiens GN=PINK1 PE=1 SV=1	[220] MMWNISAGSSSEAI LNTMSQELVPASR [246]	S228		S228	PHOS	S228	PHOS	S228	PHOS
Q15818	NPTX1_HUMAN Neuronal pentraxin-1 OS=Homo sapiens GN=NPTX1 PE=2 SV=2	[181] VNTLEEGK [188]	T183		T183		T183	PHOS	T183	
Q6ZR08	DYH12_HUMAN Dynein heavy chain 12, axonemal	[1073] VELIALIS TSAAR [1085]	S1082		S1082		S1082	PHOS	S1082	

	OS=Homo sapiens GN=DNAH12 PE=2 SV=2									
Q8IWV8	UBR2_HUMAN E3 ubiquitin-protein ligase UBR2 OS=Homo sapiens GN=UBR2 PE=1 SV=1	[355] LMLSDSK [361]	S360		S360		S360	PHOS	S360	
A0A1B0GWI3	A0A1B0GWI3_HUMAN Protein LINC01125 OS=Homo sapiens GN=LINC01125 PE=4 SV=1	[43] ASYSQQK [49]	S46		S46	PHOS	S46	PHOS	S46	PHOS

Online references:

1. Li Y, Klena NT, Gabriel GC, Liu X, Kim AJ, Lemke K, et al. Global genetic analysis in mice unveils central role for cilia in congenital heart disease. *Nature*. 2015;521:520-524
2. Hu Z, Crump SM, Zhang P, Abbott GW. Kcne2 deletion attenuates acute post-ischaemia/reperfusion myocardial infarction. *Cardiovascular research*. 2016;110:227-237
3. Caldwell JL, Smith CE, Taylor RF, Kitmitto A, Eisner DA, Dibb KM, et al. Dependence of cardiac transverse tubules on the bar domain protein amphiphysin ii (bin-1). *Circulation research*. 2014;115:986-996
4. Gong G, Song M, Csordas G, Kelly DP, Matkovich SJ, Dorn GW, 2nd. Parkin-mediated mitophagy directs perinatal cardiac metabolic maturation in mice. *Science*. 2015;350:aad2459
5. Liao X, Zhang R, Lu Y, Prosdocimo DA, Sangwung P, Zhang L, et al. Kruppel-like factor 4 is critical for transcriptional control of cardiac mitochondrial homeostasis. *The Journal of clinical investigation*. 2015;125:3461-3476
6. Ackers-Johnson M, Li PY, Holmes AP, O'Brien SM, Pavlovic D, Foo RS. A simplified, langendorff-free method for concomitant isolation of viable cardiac myocytes and nonmyocytes from the adult mouse heart. *Circulation research*. 2016;119:909-920
7. Zou MH, Kirkpatrick SS, Davis BJ, Nelson JS, Wiles WGt, Schlattner U, et al. Activation of the amp-activated protein kinase by the anti-diabetic drug metformin in vivo. Role of mitochondrial reactive nitrogen species. *The Journal of biological chemistry*. 2004;279:43940-43951
8. Schisler JC, Rubel CE, Zhang C, Lockyer P, Cyr DM, Patterson C. Chip protects against cardiac pressure overload through regulation of ampk. *The Journal of clinical investigation*. 2013;123:3588-3599
9. Kim J, Kundu M, Viollet B, Guan KL. Ampk and mtor regulate autophagy through direct phosphorylation of ulk1. *Nature cell biology*. 2011;13:132-141
10. Neumann D, Woods A, Carling D, Wallimann T, Schlattner U. Mammalian amp-activated protein kinase: Functional, heterotrimeric complexes by co-expression of subunits in escherichia coli. *Protein expression and purification*. 2003;30:230-237
11. Wang B, Zeng H, Wen Z, Chen C, Wang DW. Cyp2j2 and its metabolites (epoxyeicosatrienoic acids) attenuate cardiac hypertrophy by activating ampkalpha2 and enhancing nuclear translocation of akt1. *Aging cell*. 2016;15:940-952
12. Zhang T, Zhang Y, Cui M, Jin L, Wang Y, Lv F, et al. Camkii is a rip3 substrate mediating ischemia- and oxidative stress-induced myocardial necroptosis. *Nature medicine*. 2016;22:175-182